



Co-published by
Institute of Fluid-Flow Machinery
Polish Academy of Sciences
Committee on Thermodynamics and Combustion
Polish Academy of Sciences

Copyright©2025 by the Authors under licence CC BY-NC-ND 4.0

<http://www.imp.gda.pl/archives-of-thermodynamics/>



Performance Characteristics Investigation of a Solar Rankine Cycle Powered Air Conditioning System for Residential Buildings using Low GWP Working Fluids

Youcef Maalem^a, Hakim Madani^{b*}

^aEcole Nationale Polytechnique de Constantine (ENPC), BP75 A, Nouvelle Ville RP, 25000 Constantine, Algeria

^bLESEI, Department of Mechanical Engineering, Faculty of Technology, University of Batna 2, 05000 Batna, Algeria

*Corresponding author email: h.madani@univ-batna2.dz

Received: 02.08.2024; revised: 20.12.2024; accepted: 21.12.2024

Abstract

Screening for eco-friendly working fluids with high-energy efficiency is one of the highest challenges in the air conditioning sector. The present research aims to investigate and compare the performance characteristics of fourteen promising low global warming potential working fluids, less than 150, in solar organic Rankine cycle powered vapour compression cycle for air conditioning of residential buildings. The working fluids selected are R152a, R161, R1234yf, R1234ze(E), R1233zd(E), R290, R1270, R600a, R600, R601a, R601, R131i, RE170 and R123. The performance characteristics investigated are the organic Rankine cycle efficiency (η_{ORC}), the ratio (WRm) of network output (W_{net}) for the organic Rankine cycle to mass flow (m_{ORC}) rate for organic Rankine cycle, volumetric flow ratio (VFR), expander size parameter (SP), cooling power (Q_{eva}) of vapour compression cycle, coefficient of performance (COP_{VCC}) of vapour compression cycle, coefficient of performance (COP_s) of the organic Rankine cycle–vapour compression cycle system, the ratio ($CPRm$) of cooling power (Q_{eva}) to ($m_{ORC}+m_{VCC}$), and the total efficiency of solar air conditioning system (η_t). The investigated results proved that the working fluid RE170 (global warming potential = 1) is the most suitable working fluid for the organic Rankine cycle–vapour compression cycle system through the comprehensive comparison of η_{ORC} , WRm , VFR , SP , Q_{eva} , COP_{VCC} , COP_s , $CPRm$ and η_t for the fourteen working fluids.

Keywords: Solar Rankine cycle; Air conditioning system; Thermodynamic analysis; Performance characteristics

Vol. 46(2025), No. 1, 97–107; doi: 10.24425/ather.2025.154184

Cite this manuscript as: Maalem, Y., & Madani, H. (2024). Performance Characteristics Investigation of a Solar Rankine Cycle Powered Air Conditioning System for Residential Buildings using Low GWP Working Fluids. *Archives of Thermodynamics*, 46(1), 97–107.

1. Introduction

In recent years, environmental preservation and energy conservation have grown in significance in residential buildings [1] due to the annual energy consumption behaviour of the growing population. The steadily increasing demand in the world for cooling and heating applications is in major part met by the vapour compression systems. Furthermore, in response to increasing environmental concerns, there has been a growing focus on utilizing eco-friendly working fluids that offer high-energy efficiency.

Actually, energy systems that provide comfort, like the domestic air-conditioning system, contribute considerably to the energy consumption – electric power provided to residential buildings during the summer and especially during the peak time due to the temperature difference between the condenser and evaporator of the system [2,3].

To solve this problem, several researchers therefore have presented solutions to reduce the electricity consumption of these systems under these conditions. One of the solutions to tackle this issue is the utilization of thermal energy from clean sources of sustainable energy such as solar energy to reduce the

Nomenclature

A_{col} – solar collector aperture area, m^2
 CMR – compression ratio in compressor
 COP_s – coefficient of performance for ORC-VCC
 COP_{VCC} – coefficient of performance for VCC
 CPR_m – ratio of Q_{eva} to overall mass flows of ORC-VCC, kWs/kg
 EPR – expansion ratio in expander
 h_1 – enthalpy at expander inlet, kJ/kg
 h_{2s} – enthalpy at expander outlet based on isentropic process, kJ/kg
 h_3 – enthalpy at working fluid pump inlet, kJ/kg
 h_4 – enthalpy at working fluid pump outlet, kJ/kg
 h_{4s} – enthalpy at working fluid pump outlet based on isentropic process, kJ/kg
 h_5 – enthalpy at evaporator outlet, kJ/kg
 h_{6s} – enthalpy at compressor outlet based on isentropic process, kJ/kg
 h_7 – enthalpy at evaporator inlet, kJ/kg
 I – direct solar radiation intensity, kW/m^2
 m_{ORC} – mass flow rate for ORC, kg/s
 m_{VCC} – mass flow rate for VCC, kg/s
 P_5 – pressure at evaporator outlet, kPa
 P_6 – pressure at compressor outlet, kPa
 P_c – cooling power per collector square meter, kW/m^2
 Q_{eva} – cooling power, kW
 Q_{gen} – useful energy gained from the solar collector, kW
 SP – expander size parameter, m
 T_{amb} – ambient temperature, $^{\circ}C$
 T_{con} – condensation temperature in the condenser, $^{\circ}C$
 T_{eva} – evaporation temperature in the evaporator, $^{\circ}C$
 T_{gen} – generation temperature in the generator, $^{\circ}C$

T_m – solar collector temperature, $^{\circ}C$
 v_1 – specific volume of working fluid at expander inlet, m^3/kg
 v_2 – specific volume of working fluid at expander outlet, m^3/kg
 V_1 – volumetric flow of working fluid at expander inlet, m^3/s
 V_2 – volumetric flow of working fluid at expander outlet, m^3/s
 VFR – volumetric flow ratio
 W_{com} – compressor work input, kW
 W_{exp} – expander work output, kW
 W_{net} – net power output of ORC, kW
 W_{pump} – working fluid pump power consumption, kW
 WR_m – ratio of W_{net} to m_{ORC} , kWs/kg

Greek symbols

η_{com} – compressor isentropic efficiency
 η_{exp} – expander isentropic efficiency
 η_{ORC} – organic Rankine cycle efficiency
 η_{pump} – working fluid pump isentropic efficiency
 η_{Solar} – thermal efficiency of solar collector
 η_t – total efficiency of solar air conditioning system
 ρ_1 – density of working fluid at expander inlet, kg/m^3
 ρ_2 – density of working fluid at expander outlet, kg/m^3

Abbreviations and Acronyms

COP – coefficient of performance
 ETC – evacuated tube collectors
 FPC – flat plate collectors
 GWP – global warming potential
 ORC – organic Rankine cycle
 VCC – vapour compression cycle
 VCR – vapour compression refrigeration

electric power produced from gas turbine used for air-conditioning.

In particular in warm climate countries, such as the south of Algeria, solar radiation is the most sufficient in those areas, where it still has untapped potential, and air-conditioning systems driven by solar energy are very useful applications in these countries. These systems are economically attractive and acceptable in environmental terms. In the context of recent developments in the field of energy engineering from a building energy point of view [4], there is a lot of potential for lowering the amount of electric power used in the domestic air-conditioning system by utilizing solar thermal energy by using modern technologies [5].

Among these technologies, there are two promising energy systems for converting solar energy into processes that involve thermal comfort by use of either the absorption/adsorption refrigeration cycles or the thermo-mechanical air conditioning systems [6–8]. Although absorption and adsorption are still the dominant technologies in solar air-conditioning and cooling, the gradual removal of absorption chiller operating limits and the recent developments in organic Rankine cycle (ORC) equipment [9] to extract work from low-grade thermal sources to lower residential electric consumption [10] have sparked increasing attention in thermo-mechanical air conditioning systems.

Currently, the use of low-grade thermal sources to operate an ORC–VCC system for air-conditioning and cooling with

working fluids has become the subject of renewed interest and has been reported by many researchers.

Molés et al. [11] examined a hybrid ORC–VCR system operating under diverse conditions, powered by low-temperature heat sources and employing low global warming potential (GWP) fluids, including R134a, for both power generation and refrigeration cycles. They came to the conclusion that R1336mzz(Z) and R1234ze(E), respectively, are the best candidates for the power and refrigeration cycles.

Asim et al. [12] looked at the working fluid selection and performance of a VCR–ORC system, which recovers the waste heat. R600a-R123 was selected as the fluid pair for the integrated system based on thermodynamics (energy and exergy) and thermo-economic analysis, where the authors found that the systems combined coefficient of performance (COP) could be raised from 3.10 to 3.54.

Saleh [13] introduced novel hydrofluoroolefins alongside conventional hydrofluorocarbons as potential working fluids for an ORC–VCR system utilizing low-grade thermal energy. This integrated system combines the vapour compression refrigeration cycle with the organic Rankine cycle to enhance overall efficiency and performance. With a maximum overall performance of 0.718 at a condenser temperature of $30^{\circ}C$ and basic values for the remaining parameters, the results showed that working fluid R600 is the best candidate compared to the other substances suggested for the hybrid ORC–VCR system. Still, its flammability ought to draw sufficient notice.

Aphornratana and Sriveerakul [14] evaluated the suitability of the working fluids R22 and R134a for optimizing the heat-powered refrigeration cycle, specifically a combined Rankine–vapour–compression system. The system can be powered by low-grade thermal energy as low as 60°C and produce cooling temperatures as low as –10°C. The results showed that R134a achieves the best system performance.

A combined ORC–VCR system using R600, R600a, R245fa, and R601 as working fluids was theoretically analysed by Cihan [15]. The combined system is best suited for R601 fluid, according to the results.

Bu et al. [16] looked into six working fluids (R134a, R123, R245fa, R290, R600a, and R600) to find the best working fluids for an ORC–VCR system that is powered by geothermal energy. They concluded that R600a is the best option. Nevertheless, enough attention should be paid to R600a flammability.

Li et al. [17] investigated the performance of hydrocarbons including R290, R600, R600a and R1270 as working fluids in an ORC–VCC system. Their evaluation, considering total COP and the ratio of combined mass flow rates to cooling output, identified R600 as the optimal choice, contrasting with R1270, which emerged as the least preferred option.

Two distinct working fluids, R245fa and R134a, were used in the study of an ORC–VCR system by Wang et al. [18] for the organic Rankine cycle and conventional vapour compression cycle, respectively. The system's overall coefficient of performance was close to 0.50.

In the study of Yue et al. [19], the authors investigated the performance of an ORC integrated with a car air conditioning system using cyclopentane, pentane, R134a and R245fa as working fluids. Their findings indicate that, among the studied conditions, R134a demonstrated superior thermal and economic performance compared to the other fluids considered.

The combined ORC–VCR thermodynamic model was developed by Hu et al. [20] for ship air conditioning in order to effectively use cooling water and transfer waste heat from flue gases. Using five widely used working fluids (R22, R141b, R236ea, R218 and R601), the system performance was examined. It was determined through calculations that R601 was the best working fluid.

Eight working fluids (R290, R717, R600, R600a, R143a, R22, R152a and R142a) were used in an ORC–VCR system that was activated by low-grade sensible energy, according to Kim and Perez-Blanco's analysis [21]. The fluids were arranged in order of critical temperature. The findings showed that because of its relatively high efficiencies, R600a provides a sensitivity analysis in a few unique situations.

The thermal performance analysis of an ORC–VCR system with a common shaft was the focus of the study of Khatoun et al. [22]. Two refrigerants (R245fa and R290), were selected for the organic Rankine cycle and three (R245fa, R123 and R134a) were chosen for the vapour compression cycle. With propane serving as the working fluid in the organic Rankine cycle and R123 serving as the working fluid in the vapour compression cycle. The results indicated the highest efficiency of 16.48% and the highest coefficient of performance value of 2.85 at 40°C.

In order to determine which refrigerant would be best for the

ORC–VCR system, Jeong and Kang [23] tested R123, R134a and R245ca. The R123 case has the highest thermal efficiency, it has been discovered.

Küçük and Kılıç [24] investigated a hybrid ORC–VCR system functioning under various conditions to generate power and cooling. The analysis employs the working fluids R114, R123, R600, R600a and R245fa in the ORC system, and R141b, R600a, R290, R134a, R123, R245fa and R143a in the VCRC subsystem. The results indicated that the R123–R141b fluid pair yields the optimal values for energy utilization factor, exergy efficiency, system coefficient of performance and net power.

In the research conducted by Wang et al. [25], the authors evaluated the performance of the ORC–VCR system utilizing a zeotropic mixture of R245fa/R134a (0.9/0.1) under diverse evaporation temperatures and cooling conditions. The interaction between cooling water temperature and flow rate on the performance of the ORC–VCR system is examined. They determined that the temperature of the cooling water exerts a more significant influence on the operational characteristics of the system than the flow rate of the cooling water. As the temperature of the cooling water decreases and its flow rate increases, the system's cooling capacity rises, whereas the coefficient of performance remains relatively stable.

Qureshi et al. [26] examined the performance of refrigeration systems using solar-based organic Rankine cycle (ORC) and vapour compression refrigeration (VCR) cycles. Dry natural hydrocarbons like n-decane, n-dodecane and toluene are used in ORC, while traditional working fluids like ethane, propane, isobutane, isopentane and isohexane are used in VCR due to environmental concerns. The study found that solar thermal energy could be efficiently operated within 90°C to 315°C, reducing the need for conventional fossil fuels.

Al-Sayyab et al. [27] studied the performance of a modified organic Rankine–vapour compression cycle using ultra-low GWP fluids (R1234ze(E), R1243zf, and R1234yf). The system configured for three operational modes, significantly improved refrigerant efficacy. The R1234ze(E) power-cooling mode showed the highest COP increase, while incorporating a recapture heat exchanger improved power generation by 58%.

Based on the literature reviewed, consensus has yet to be reached on the optimal working fluid for ORC–VCR systems. Consequently, further research investigating the performance of working fluids in ORC–VCR systems remains necessary.

This study proposes and addresses to utilize the untapped potential of solar energy in warm climate countries, such as the south of Algeria for the operation of an ORC–VCC system by using the solar thermal collector, which is energy efficient in the application of air conditioning for residential buildings. The study contributes to the research of an optimal eco-friendly working fluid for the solar driven ORC–VCC system and the study of its performance characteristics. Therefore, fourteen promising working fluids have GWP less than 150 are investigated and compared under the same operating conditions to identify suitable fluids which may yield high system efficiencies.

The working fluids investigated are R152a, R161, R1234yf, R1234ze(E), R1233zd(E), R290, R1270, R600a, R600, R601a, R601, R131I, RE170 and R123.

Table 1. Candidate working fluids and their basic properties [28,29].

| Substance | Chemical formula | Physical properties data | | | | | Environmental data | | Safety data |
|------------|---|--------------------------|---------------|--------------------|---------------------|--|--------------------|-------|-----------------|
| | | M (g/mol) | NBP (°C) | T_{crit} (°C) | P_{crit} (MPa) | $v_{crit} \times 10^3$ (m ³ /kg) | GWP 100 yr | ODP | Safety group |
| R152a | CH ₃ -CHF ₂ | 66.05 | -24.0 | 113.3 | 4.517 | 2.72 | 133 | 0 | A2 |
| R161 | C ₂ H ₅ F | 48.1 | -37.6 | 102.1 | 5.010 | 3.31 | 12 | 0 | A3 |
| R1234yf | CF ₃ CF=CH ₂ | 114.0 | -29.5 | 94.7 | 3.38 | 2.10 | 4 | 0 | A2L |
| R1234ze(E) | CHF=CHCF ₃ | 114.0 | -18.9 | 109.4 | 3.635 | 2.04 | 6 | 0 | A2L |
| R1233zd(E) | CHCL=CH-CF ₃ | 130.5 | 18.3 | 165.6 | 3.57 | 2.10 | 7 | 0 | A1 |
| RE170 | CH ₃ -O-CH ₃ | 46.1 | -24.8 | 127.2 | 5.34 | 3.65 | 1 | 0 | A3 |
| R290 | C ₃ H ₈ | 44.10 | -42.1 | 96.7 | 4.25 | 4.58 | ~20 | 0 | A3 |
| R1270 | CH ₃ -CH=CH ₂ | 42.08 | -47.7 | 92.4 | 4.67 | 4.58 | <20 | 0 | A3 |
| R600a | iso-C ₄ H ₁₀ | 58.12 | -11.7 | 134.7 | 3.63 | 4.46 | ~20 | 0 | A3 |
| R600 | C ₄ H ₁₀ | 58.12 | -0.55 | 152.0 | 3.80 | 4.39 | ~20 | 0 | A3 |
| R601a | CH ₃ CH ₂ CH(CH ₃) ₂ | 72.15 | 27.8 | 187.2 | 3.38 | 4.24 | 4 | 0 | A3 |
| R601 | CH ₃ (CH ₂) ₃ CH ₃ | 72.15 | 36.1 | 196.6 | 3.37 | 4.31 | 4 | 0 | A3 |
| R1311 | CF ₃ I | 195.9 | -21.9 | 123.3 | 3.953 | 1.15 | 0 | 0 | A1 |
| R123 | CHCl ₂ CF ₃ | 152.93 | 27.5 | 183.68 | 3.67 | 1.81 | 90 | 0.020 | B1 |

The basic properties of the candidate working fluids are given in Table 1. In this regard, the environmental impact of the working fluids is considered as the most important criterion [28,29].

2. System description

The schematic diagram of the solar driven ORC–VCC system under investigation is shown in Fig. 1(a). It comprises a base ORC (1-2-3-4-1) and a base VCC (5-6-3-7-5). The overall system consists of a solar collector (generator), an expander, a con-

denser, a feed pump, a compressor, a throttle valve and an evaporator. A single shaft between the expander and compressor joins the two cycles together. This system has an integrated configuration and uses the same working fluid in both cycles to minimize the problem associated with leaking of the working fluids.

Fig. 1(b) shows the T – s diagram of the solar driven ORC–VCC system. This system has eight fundamental transformations occurring during thermodynamic cycles (ORC and VCC), and the ORC and VCC condensation processes take place in a shared condenser at the same pressure.

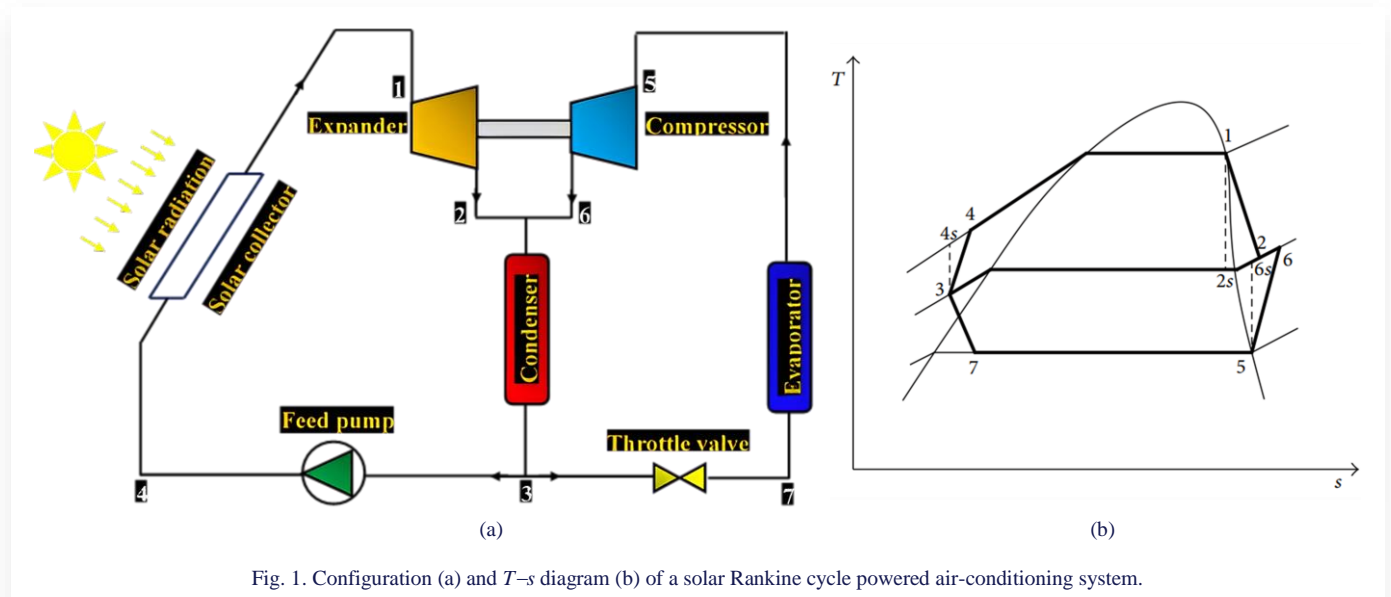


Fig. 1. Configuration (a) and T – s diagram (b) of a solar Rankine cycle powered air-conditioning system.

The operation processes of the subsystems ORC and VCC are described as follows:

- Process 1→2s: is an isentropic expansion process across the expander of ORC.
- Process 1→2: is the actual expansion process.
- Process 2→3: is a heat rejection (condensation) process across the condenser of ORC and VCC.
- Process 3→4s: is an isentropic pumping process across the pump of ORC.
- Process 3→4: is the actual pumping work.
- Process 4→1: is a heat addition process in the solar collector (generator) of ORC.
- Process 5→6s: is an isentropic compression across the compressor of VCC.
- Process 5→6: is the actual compression process.
- Process 6→3: is a heat rejection (condensation) process across the condenser of ORC and VCC.
- Process 3→7: is an isenthalpic expansion across the throttle valve of VCC.
- Process 7→5: is a heat absorption (evaporation) in the evaporator of VCC.

The working principle of this system is described below:

- In the ORC, the liquid working fluid is pressurized by the feed pump and sent into the solar collector to exchange heat with the solar energy to vaporize into high-temperature and high-pressure vapour (*process 4→1*). Then, high-pressure vapour drives an expander attached to a vapour compressor to do mechanical work (*process 1→2*). Following that operation, the vapour working fluid at the expander outlet is combined with the vapour working fluid at the compressor outlet, going through the condenser and cooling to a low-temperature and low-pressure liquid state (*process 2→3*). To finish a cycle process, the liquid working fluid eventually returns to the feed pump (*process 3→4*).
- In the subsystem VCC, after being depressurized by the throttle valve, the low-temperature and low-pressure liquid enters the evaporator and exchanges with air for heat exchange (*process 7→5*). Following heat exchange, the working fluid enters the compressor and is compressed into high pressure and temperature (*process 5→6*). It is mixed with the working fluid at the outlet of the expander in ORC, and then enters the condenser, where it is cooled to a liquid state (*process 6→3*). To finish a cycle process (*processes 3→7*), the liquid working fluid finally goes through the throttle valve once more.

3. Thermodynamic analysis

3.1. Assumptions

To perform the analysis of the solar driven ORC–VCC, the following assumptions are applied for modelling:

- The system works under steady state conditions.
- Solar collector (generator) has a uniform radial temperature distribution.
- No pressure losses in connection tubes and heat exchangers.
- The transformations in heat exchangers are isobaric.
- The working fluid leaving the generator, evaporator and condenser is assumed to be saturated.
- The variations in kinetic and potential energy are not considerable.
- The fluid undergoes a constant enthalpy process in the throttle valve (isenthalpic process) of the subsystem VCC.
- The work produced by the expander of the subsystem ORC is equal to the work consumed by the compressor of the subsystem VCC.
- The isentropic efficiencies of the pump (η_{pump}), expander (η_{exp}) and compressor (η_{com}) have a given value and are not affected by operating conditions.

Based on the above assumptions and referring to the system under investigation presented in Fig. 1, the thermodynamic models are developed and mentioned below.

3.2. Cycle modelling

This section presents the mathematical description of the solar driven ORC–VCC system.

Evacuated tube collectors (ETC) are used for solar heat collecting, considering their relatively higher performance compared to flat plate collectors (FPC) under low and medium temperatures [30]. The model of heat-collecting efficiency of ETC is described by Eq. (1) [31]:

$$\eta_{Solar} = a_0 - a_1 \frac{(T_m - T_{amb})}{I} - a_2 \frac{(T_m - T_{amb})^2}{I}, \quad (1)$$

where $a_0 = 0.721$, $a_1 = 0.89$ and $a_2 = 0.0199$ are the solar collector efficiency constants, a_0 is the efficiency of the collector, and a_1 and a_2 are the first and second heat loss coefficients. Here, T_m means the temperature of working fluid in the collector and T_{amb} means the ambient temperature. I represents the incident solar radiation per unit area of the collector about 4.8 kWh/m² for an Algerian climate location [32].

The calculation formulas of the components of the ORC subsystem are shown as follows:

- the output work of the expander can be expressed as:

$$W_{exp} = m_{ORC}(h_1 - h_{2s})\eta_{exp}; \quad (2)$$

- the required power to the pump is expressed by:

$$W_{pump} = \frac{m_{ORC}(h_{4s} - h_3)}{\eta_{pump}}; \quad (3)$$

- the useful energy gained from the solar collector (generator) is given by:

$$Q_{gen} = m_{ORC}(h_1 - h_4); \quad (4)$$

- the net power output of the ORC subsystem is defined as:

$$W_{net} = W_{exp} - W_{pump}; \quad (5)$$

- the net power output per unit mass flow rate of working fluid of the ORC subsystem:

$$WRm = \frac{W_{net}}{m_{ORC}} = \frac{W_{exp} - W_{pump}}{m_{ORC}}; \quad (6)$$

- the volumetric flow ratio is given by:

$$VFR = \frac{V_2}{V_1}, \quad (7)$$

with:

$$V_1 = \frac{m_{ORC}}{\rho_1}, \quad (8)$$

$$V_2 = \frac{m_{ORC}}{\rho_2}; \quad (9)$$

- the expander size parameter is defined as:

$$SP = \frac{\sqrt{V_2}}{\sqrt[4]{1000(h_1 - h_{2s})}}; \quad (10)$$

- the expansion ratio across the expander is given by:

$$EPR = \frac{v_2}{v_1}; \quad (11)$$

- the thermal efficiency of the ORC subsystem is defined as:

$$\eta_{ORC} = \frac{W_{net}}{Q_{gen}} \quad (12)$$

The calculation formulas of the components of the VCC subsystem are shown as follows:

- the output power of the expander is equal to the input power of the compressor:

$$W_{com} = W_{exp}, \quad (13)$$

$$W_{com} = \frac{m_{VCC}(h_5 - h_{6s})}{\eta_{com}}, \quad (14)$$

- the cooling capacity of the VCC subsystem produced from the solar energy is calculated by:

$$Q_{eva} = m_{VCC}(h_5 - h_7), \quad (15)$$

with:

$$m_{VCC} = \frac{W_{com}\eta_{com}}{(h_5 - h_{6s})}, \quad (16)$$

- the compression ratio across the compressor is given by:

$$CMR = \frac{P_6}{P_5}, \quad (17)$$

- the coefficient of performance the VCC subsystem is given by:

$$COP_{VCC} = \frac{Q_{eva}}{W_{com}}, \quad (18)$$

The calculation formulas of the performance indicators of the ORC–VCC system are shown as follows:

- the coefficient of performance for the ORC–VCC system is given by:

$$COP_S = \eta_{ORC}COP_{VCC}; \quad (19)$$

- the ratio of Q_{eva} to overall mass flows of the ORC–VCC system is calculated by:

$$CPRm = \frac{Q_{eva}}{m_{ORC} + m_{VCC}}; \quad (20)$$

- the overall thermal efficiency of the solar driven ORC–VCC system is defined as:

$$\eta_t = \eta_{Solar}COP_S; \quad (21)$$

- the cooling power per square meter of the collector is calculated as follows:

$$PC = \frac{Q_{eva}}{A_{col}} \quad (22)$$

Based on the theoretical model presented above, a simulation code is developed to simulate the performance characteristics of the solar driven ORC–VCC system with various working fluids.

The input values of operating parameters are listed in Table 2.

Table 2. Condition of simulation for the solar driven ORC–VCC system.

| Parameter | Symbol | Typical value | Range |
|----------------------------------|---------------|-----------------------|---------|
| Working fluid mass flow in ORC | m_{ORC} | 1.0 kg/s | – |
| Evaporation temperature | T_{eva} | –5°C | – |
| Generation exit temperature | T_{gen} | 80°C | 60–90°C |
| Condensation temperature | T_{con} | 40°C | – |
| Ambient temperature | T_{amb} | 40°C | – |
| Compressor isentropic efficiency | η_{com} | 80 | – |
| Expander isentropic efficiency | η_{exp} | 85 | – |
| Pump isentropic efficiency | η_{pump} | 90 | – |
| Solar radiation intensity | I | 1000 W/m ² | – |

4. Results and discussion

4.1. Model validation

Before presenting the results of thermodynamic analysis, a brief discussion on validation of the present calculating program for system simulation would be appropriate.

Due to their similar integrated cycle configuration, data of Li et al. [17] are used as a reference for comparisons. Since the organic Rankine cycle is driven by a boiler instead of a solar collector in the reference, the product of coefficient of performance for ORC–VCC system is used as the index parameter for comparison under the same operating conditions ($m_{ORC} = 1$ kg/s, $T_{eva} = 5^\circ\text{C}$, $T_{con} = 40^\circ\text{C}$, $T_{boil} = 60\text{--}90^\circ\text{C}$, $\eta_{exp} = 0.80$, $\eta_{com} = 0.75$ and $\eta_{pump} = 0.75$) and working fluids (R290, R600, R600a and R1270). Based on different boiler temperatures, Fig. 2 compares the product of the coefficient of performance for the ORC–VCC system between the current work and the reference.

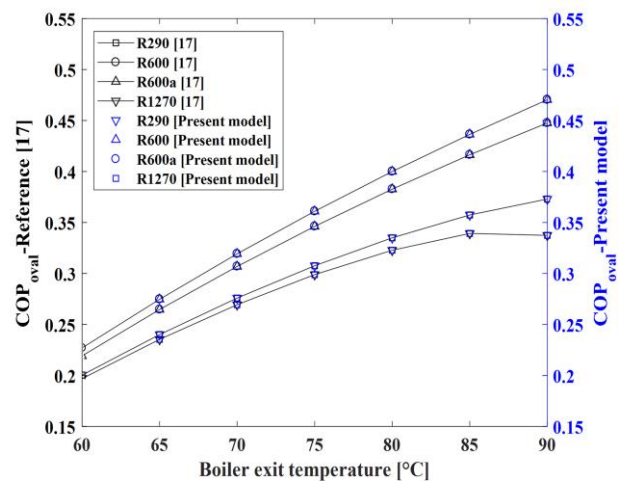


Fig. 2. Validation of the calculation model.

The comparison of results indicates a very good agreement between the results, which confirms the validity of our simulation model.

4.2. Performance characteristics

This section illustrates the strategy presented on working fluid selection in our case study. We propose to assess the performance characteristics of the solar-powered ORC–VCC with a temperature that ranges between 60–90°C and 1000 W/m² of beam solar radiation.

4.2.1. Influence of working fluid types on ORC subsystem

The influence of generation temperature (T_{gen}) on the parameters (η_{ORC} , WRm , VRF and SP) of ORC driven by solar energy using the investigated working fluids, while keeping the other operating conditions constant are presented in Figs. 3–6.

Figure 3 illustrates the influence of generation temperature (T_{gen}) on organic Rankine cycle efficiency (η_{ORC}) of the working fluids, namely R152a, R161, R1234yf, R1234ze(E), R1233zd(E), R290, R1270, R600a, R600, R601a, R601, R131I, RE170 and R123.

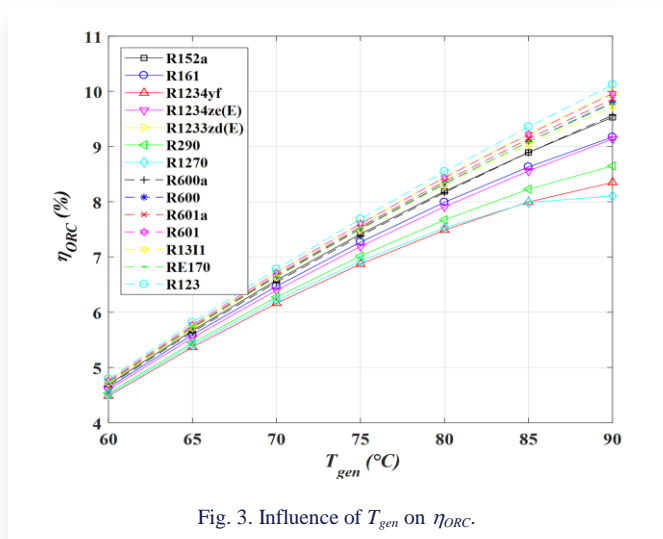


Fig. 3. Influence of T_{gen} on η_{ORC} .

It can be found from the figure profiles that the thermal efficiency of ORC depends largely on heat source temperatures, where it increases with the increase of T_{gen} for all investigated working fluids. This is because the increase of generation temperature results in enhancement of the heat added to the generator (Q_{gen}), which increases the thermal efficiency.

By comparing the simulation results of the thermal efficiency obtained for each working fluid, it can be seen that the differences in thermal efficiency between every working fluid are negligible when $T_{gen} < 70^\circ\text{C}$. However, at $T_{gen} > 70^\circ\text{C}$, the differences get noticeable, where it is obvious that the working fluid R123 exhibits the highest thermal efficiency among the investigated working fluids, followed by R601, R1233zd(E), R601a and RE170, whereas R1234yf and R1270 have the minimum thermal efficiency.

Figure 4 shows the effects of the generation exit temperature on the ratio WRm of ORC driven by solar energy using the working fluids R152a, R161, R1234yf, R1234ze(E), R1233zd(E), R290, R1270, R600a, R600, R601a, R601, R131I, RE170 and R123.

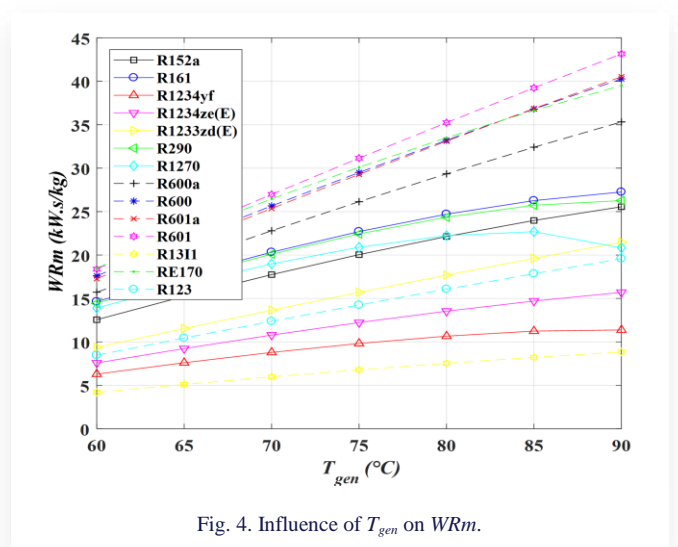


Fig. 4. Influence of T_{gen} on WRm .

The ratio WRm is defined as the ratio of net power output (W_{net}) of ORC to the ORC mass flow rate, reflecting the power capability of the working fluid per unit mass flow rate.

It can be found from the profiles of Fig. 4 that WRm exhibits the same behaviour as the thermal efficiency (η_{ORC}), where it rises as T_{gen} rises for every working fluid that has been studied. This is because, when the condensation temperature (T_{con}) is constant, h_{4s} and h_3 remain unchanged, but the difference between h_1 and h_{2s} increases with increasing T_{gen} , which causes WRm to increase.

By comparing the simulation results of WRm obtained for each working fluid, it can be found that R601 exhibits the highest WRm among the investigated working fluids, followed by RE170, R600 and R601a, whereas R131I and R1234yf have the minimum WRm under the generation temperature range considered.

The effect of generation temperature (T_{gen}) on VFR is illustrated in Fig. 5. The VFR is defined as the specific volume variation across the expander in an isentropic process, which accounts for the effect of compressibility through the expansion.

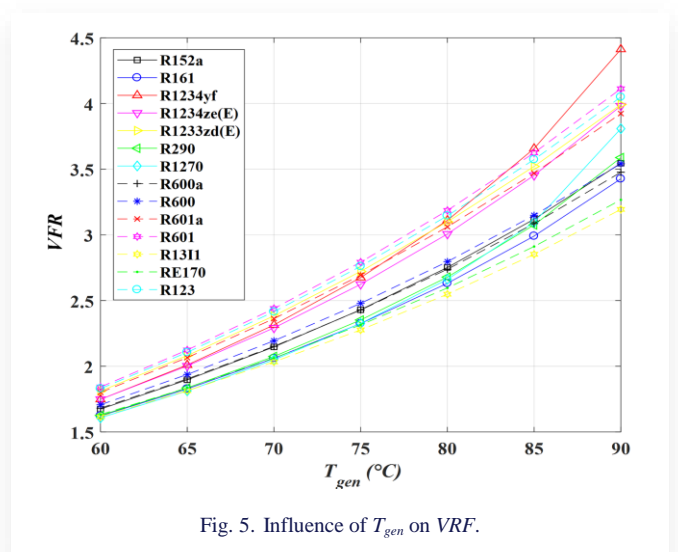


Fig. 5. Influence of T_{gen} on VFR .

As it is seen from Fig. 5, with the increase of T_{gen} , VFR for all working fluids increases. Examining the profiles of VFR for each working fluid in the figure, it can be found that the working fluids R601, R123 and R1233zd(E) have the highest VFR , while the working fluids R161, RE170, R600a and R131I have the lowest VFR . The low VFR leads to high η_{ORC} . This result is in line with what Macchi and Perdichizzi [33] found.

Macchi and Perdichizzi [33] state that higher turbine efficiency is produced by lower VFR values. Furthermore, according to Invernizzi et al. [34], the VFR needs to be less than 50 in order to attain a turbine efficiency of more than 80%. Since the VFR for all working fluids in this study is less than 4.5, a turbine efficiency of more than 80 % may be attained.

The variation of the expander size parameter (SP) with (T_{gen}) is plotted and presented in Fig. 6. According to Lakew and Bolland [35]; Stijepovic et al [36], SP is a measure of expander size that corresponds to the real expander size.

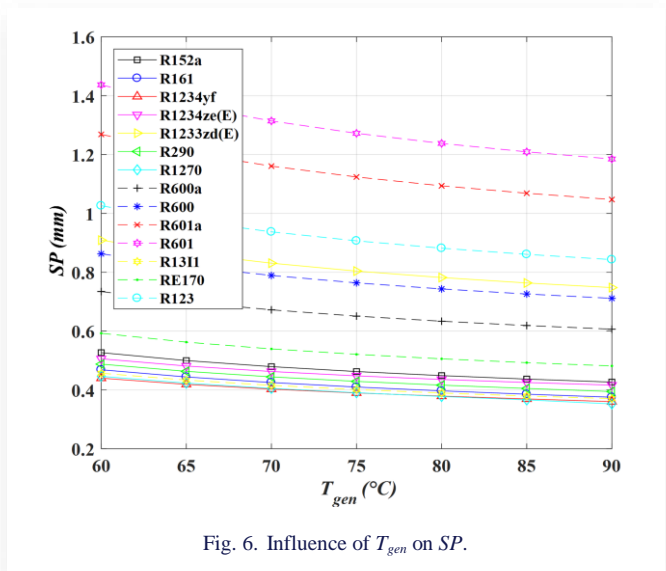


Fig. 6. Influence of T_{gen} on SP .

As it is seen from the figure, with the increase of generation temperature, SP for all working fluids decreases. This is explained by the fact that, according to Eq. (10), a higher generation temperature causes a greater enthalpy drop between the expander's inlet and outlet in addition to increasing thermal efficiency and resulting in a lower SP .

By comparing the simulation results of SP obtained for each working fluid, it can be observed that at all heat source temperatures, the working fluids R601, R601a and R123 have the highest SP , while the working fluids R1234yf, R1270, R161, R131I, R1234ze(E), R152a and RE170) have the lowest SP .

According to Eq. (10), the working fluids R1234yf, R1270, R161, R131I, R1234ze(E), R152a and RE170 have a higher pressure and density at the expander outlet, which lowers the volumetric flow of working fluids at the expander outlet (V_2), and consequently SP .

From the discussion above, it is evident that working fluid RE170 is the most suitable working fluid among the fourteen examined working fluids for ORC in the heat source temperature range of 60–90°C in terms of η_{ORC} , WRm , VFR and SP .

4.2.2. Influence of working fluid types on VCC subsystem

The influence of generation temperature (T_{gen}) on the parameters (Q_{eva} and COP_{VCC}) of VCC using the investigated working fluids while keeping the other operating conditions constant are presented in Figs. 7–8.

Figure 7 illustrates the influence of generation temperature (T_{gen}) on cooling power (Q_{eva}) of the working fluids, namely R152a, R161, R1234yf, R1234ze(E), R1233zd(E), R290, R1270, R600a, R600, R601a, R601, R131I, RE170 and R123. It can be found from the figure profiles that the cooling power of the vapour compression cycle (VCC) depends largely on heat source temperatures, where it increases with the increase of T_{gen} for all investigated working fluids.

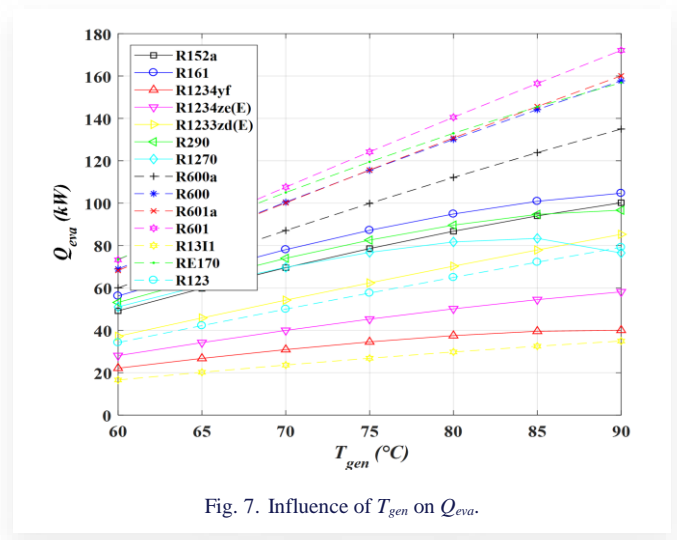


Fig. 7. Influence of T_{gen} on Q_{eva} .

By comparing the simulation results of the cooling power obtained for each working fluid, it can be seen that the working fluid R601 exhibits the highest cooling power among the investigated working fluids, followed by RE170, R600 and R601a, while R1234yf and R131I have the minimum cooling power.

The comparison of cycle performance COP_{VCC} among the 14 candidate refrigerants is illustrated in Fig. 8.

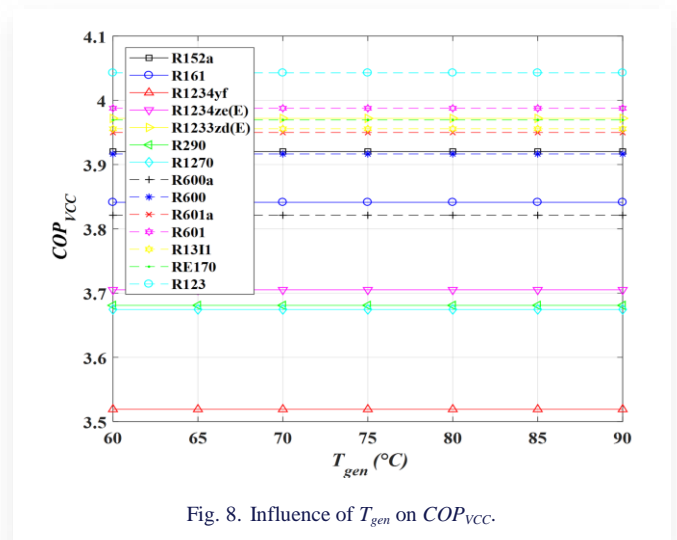


Fig. 8. Influence of T_{gen} on COP_{VCC} .

By comparing the simulation results of the coefficient of performance (COP_{VCC}) obtained for each working fluid, it can be seen that the working fluid R123 exhibits the highest coefficient of performance among the investigated working fluids, followed by R601, R1233zd(E) and RE170, while R1234yf, R1270 and R290 have the minimum coefficient of performance.

From the discussion above, it is evident that working fluids RE170 and R601 are the most suitable working fluids among the fourteen examined working fluids for the VCC system in the heat source temperature range of 60–90°C in terms of Q_{eva} and COP_{VCC} .

4.2.3. Influence of working fluid types on solar driven ORC–VCC system

The influence of generation temperature (T_{gen}) on the parameters COP_s , $CPRm$ and η_t of the ORC–VCC system using the investigated working fluids while keeping the other operating conditions constant are presented below in Figs. 9–11.

Figure 9 represents the effect of the generation temperature on the coefficient of performance (COP_s) of the ORC–VCC system using R152a, R161, R1234yf, R1234ze(E), R1233zd(E), R290, R1270, R600a, R600, R601a, R601, R1311, RE170 and R123 as working fluids. It is observed from the figure that the coefficient of performance (COP_s) of each working fluid increases with the increase in generation temperature.

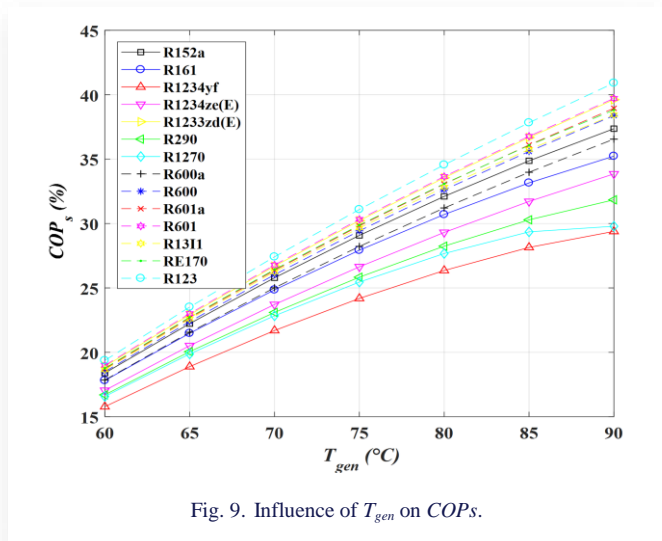


Fig. 9. Influence of T_{gen} on COP_s .

By comparing COP_s of the investigated working fluids, it would be observed that R123 exhibits the highest COP_s among the investigated working fluids, followed by R601, R1233zd(E), R601a, and RE170, while R1234yf and R1270 have the minimum COP_s . This higher COP_s of R123, R601, R1233zd(E), R601a and RE170 is due the fact that the working fluids have higher values of η_{ORC} as evident in Fig. 2 and COP_{VCC} in Fig. 8, thus leading to the highest COP_s for R123, R601, R1233zd(E), R601a and RE170 in Fig. 9.

The influence of generation temperature on $CPRm$ is shown in Fig. 10. The $CPRm$ is defined as the ratio of Q_{eva} to $(m_{ORC} + m_{VCC})$, which reflects the refrigerating capacity of the working fluid per unit mass flow rate.

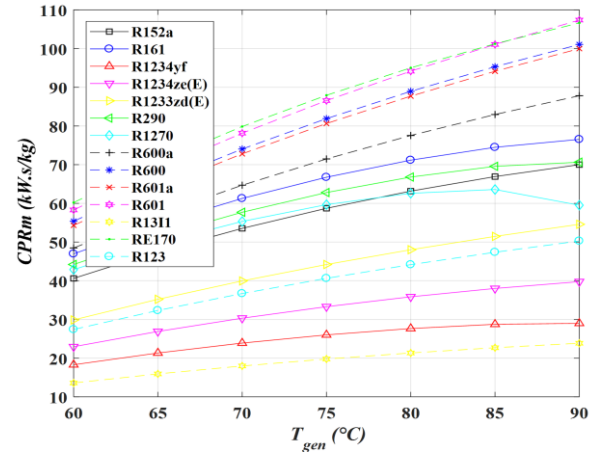


Fig. 10. Influence of T_{gen} on $CPRm$.

As it is seen from the figure with the increase of generation temperature, the profiles of $CPRm$ for all working fluids increase. By comparing, the simulation results obtained for $CPRm$ for investigated working fluids, it can be found that RE170 exhibits the highest $CPRm$ among the investigated working fluids, followed by R601, R600 and R601a, while R1234yf and R1311 have the minimum $CPRm$.

Figure 11 illustrates the influence of generation temperature (T_{gen}) on the total efficiency of the solar air conditioning system (η_t) using the investigated working fluids.

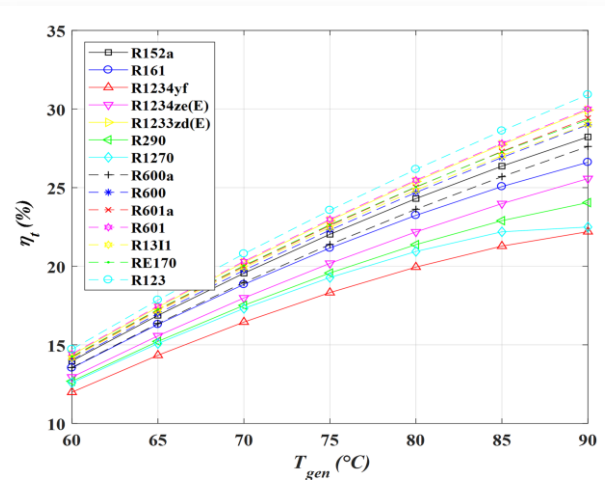


Fig. 11. Influence of T_{gen} on η_t .

It can be found from the figure profiles that the total efficiency of the ORC–VCC system depends largely on heat source temperatures, where it increases with the increase of T_{gen} for all investigated working fluids.

It is obvious that R123 exhibits the highest total efficiency among the investigated working fluids, followed by R601, R1233zd(E), R601a and RE170, while R1234yf and R1270 have the minimum total efficiency.

From the discussion above, it is evident that the working fluids R601, R601a, R1233zd(E) and RE170 are the most suitable

working fluids among the fourteen examined working fluids for the ORC–VCC system in the heat source temperature range of 60–90°C in terms of $COPs$, $CPRm$ and η_i .

5. Conclusions

In the present work, theoretical investigations of the performance characteristics were performed for a solar ORC powered VCC for an air conditioning system for residential buildings operating with low GWP working fluids, less than 150, in both cycles (ORC and VCC).

Fourteen promising working fluids R152a, R161, R1234yf, R1234ze(E), R1233zd(E), R290, R1270, R600a, R600, R601a, R601, R13I1, RE170 and R123 were selected and compared under the same operating conditions to identify the suitable working fluid which may yield the high system efficiency.

The performance characteristics studied include the organic Rankine cycle efficiency (η_{ORC}), the ratio (WRm) of net power output (W_{net}) for ORC to mass flow (m_{ORC}) rate for ORC, volumetric flow ratio (VFR), expander size parameter (SP), cooling power (Q_{eva}) of VCC, coefficient of performance (COP_{VCC}) of VCC, coefficient of performance ($COPs$) of the ORC–VCC system, the ratio ($CPRm$) of cooling power (Q_{eva}) to ($m_{ORC}+m_{VCC}$), and the total efficiency of solar air conditioning system (η_i).

Based on the results obtained from the present study, the main conclusions are listed as follows:

- The variation in the generation temperature has a significant impact on the performance characteristics of the solar ORC–VCC system.
- The performance parameters η_{ORC} , WRm , VFR , Q_{eva} , $COPs$, $CPRm$ and η_i of investigated working fluids increase with the increasing of generation temperature.
- The expander size parameter (SP) of investigated working fluids decreases with the increasing generation temperature.
- The coefficient of performance (COP_{VCC}) of the VCC is unaffected by variations in the generation temperature.
- In terms of the parameter η_{ORC} of the ORC, the working fluids R601, R1233zd(E), R601a and RE170 have the maximum η_{ORC} among the fourteen examined working fluids in the heat source temperature range of 60–90°C.
- In terms of the parameter WRm of the ORC, the working fluids R601, RE170, R600 and R601a have the maximum WRm among the fourteen examined working fluids in the heat source temperature range of 60–90°C.
- In terms of the parameter VFR of the ORC, the working fluids R161, RE170, R600a and R13I1 have the lowest VFR among the fourteen examined working fluids in the heat source temperature range of 60–90°C.
- In terms of the parameter SP of the ORC, the working fluids R1234yf, R1270, R161, R13I1, R1234ze(E), R152a and RE170 have the lowest SP among the fourteen examined working fluids in the heat source temperature range of 60–90°C.
- In terms of the parameter Q_{eva} of the VCC, the working fluids R601, RE170, R600 and R601a have the maximum

Q_{eva} among the fourteen examined working fluids in the heat source temperature range of 60–90°C.

- In terms of the parameter COP_{VCC} of the VCC, the working fluids R123, R601, R1233zd(E) and RE170 have the maximum COP_{VCC} among the fourteen examined working fluids in the heat source temperature range of 60–90°C.
- In terms of the parameter $COPs$ of the ORC–VCC system, the working fluids R123, R601, R1233zd(E), R601a and RE170 have the maximum $COPs$ among the fourteen examined working fluids in the heat source temperature range of 60–90°C.
- In terms of the parameter $CPRm$ of the ORC–VCC system, the working fluids RE170, R601, R600 and R601a have the maximum $CPRm$ among the fourteen examined working fluids in the heat source temperature range of 60–90°C.
- In terms of the parameter η_i of the ORC–VCC system, the working fluids R601, R1233zd(E), R601a and RE170 have the maximum η_i among the fourteen examined working fluids in the heat source temperature range of 60–90°C.

By analysing the performance characteristics of investigated working fluids, the investigated RE170 fluid emerges with the best performances in most of the cases, which confirms that it could be a promising working fluid in terms of performance characteristics for ORC–VCC system.

Overall, from the view point of the performance characteristics and GWP, the working fluid RE170 ($GWP = 1$) is the most suitable working fluid for the ORC–VCC system through the comprehensive comparison of η_{ORC} , WRm , VFR , SP , Q_{eva} , COP_{VCC} , $COPs$, $CPRm$ and η_i for the fourteen working fluids.

References

- [1] Maalem, Y., Fedali, S., Madani, H., & Tamene, Y. (2020). Performance analysis of ternary azeotropic mixtures in different vapor compression refrigeration cycles. *International Journal of Refrigeration*, 119, 139–151. doi: 10.1016/j.ijrefrig.2020.07.021
- [2] Li, C., Zhou, J., Cao, Y., Zhong, J., Liu, Y., Kang, C., & Tan, Y. (2014). Interaction between urban microclimate and electric air-conditioning energy consumption during high temperature season. *Applied Energy*, 117, 149–156. doi: 10.1016/j.apenergy.2013.11.057
- [3] Martins, M., Mauran, S., Stitou, D., & Neveu, P. (2012). A new thermal hydraulic process for solar cooling. *Energy*, 41, 104–112. doi: 10.1016/j.energy.2011.05.030
- [4] Maalem, Y., & Madani, H. (2024). Energetic performance investigation of ejector air conditioning cycles using the environment friendly gas R161 (Fluoroethane) as substitute to the phase-out R22 (Chlorodifluoromethane). *International Journal of Thermofluid Science and Technology*, 11, 110201. doi: 10.36963/IJTST.2024110201
- [5] Zeyghami, M., Goswami, D.Y., & Stefanakos, E. (2015). A review of solar thermo-mechanical refrigeration and cooling methods. *Renewable and Sustainable Energy Reviews*, 51, 1428–1445. doi: 10.1016/j.rser.2015.07.011
- [6] Egrican, A. N., & Karakas, A. (1986). Second law analysis of a solar powered Rankine cycle/vapor compression cycle. *Journal of Heat Recovery Systems*, 6, 135–141. doi: 10.1016/0198-7593(86)90073-1
- [7] Louajari, M., Mimet, A., & Ouammi, A. (2011). Study of the effect of finned tube adsorber on the performance of solar driven

- adsorption cooling machine using activated carbon-ammonia pair. *Applied Energy*, 88, 690–698. doi: 10.1016/j.apenergy.2010.08.032
- [8] Luo, H., Wang, R., & Dai, Y. (2010). The effects of operation parameter on the performance of a solar-powered adsorption chiller. *Applied Energy*, 87, 3018–3022. doi: 10.1016/j.apenergy.2010.03.013
- [9] Quoilin, S., Orosz, M., Hemond, H., & Lemort, V. (2011). Performance and design optimization of a low-cost solar organic Rankine cycle for remote power generation. *Solar Energy*, 85, 955–966. doi: 10.1016/j.solener.2011.02.010
- [10] Tchanche, B.F., Lambrinos, G., Frangoudakis, A., & Papadakis, G. (2011). Low-grade heat conversion into power using organic Rankine cycles – A review of various applications. *Renewable and Sustainable Energy Reviews*, 15, 3963–3979. doi: 10.1016/j.rser.2011.07.024
- [11] Molés, F., Navarro-Esbrí, J., Peris, B., Mota-Babiloni, A., & Kontomaris, K. (2015). Thermodynamic analysis of a combined organic Rankine cycle and vapor compression cycle system activated with low temperature heat sources using low GWP fluids. *Applied Thermal Engineering*, 87, 444–453. doi: 10.1016/j.applthermaleng.2015.04.083
- [12] Asim, M., Leung, M.K.H., Shan, Z., Li, Y., Leung, D.Y.C., & Ni, M. (2017). Thermodynamic and Thermo-economic Analysis of Integrated Organic Rankine Cycle for Waste Heat Recovery from Vapor Compression Refrigeration Cycle. *Energy Procedia*, 143, 192–198. doi: 10.1016/j.egypro.2017.12.670
- [13] Saleh, B. (2016). Parametric and working fluid analysis of a combined organic Rankine-vapor compression refrigeration system activated by low-grade thermal energy. *Journal of Advanced Research*, 7, 651–660. doi: 10.1016/j.jare.2016.06.006
- [14] Aphornratana, S., & Sriveerakul, T. (2010). Analysis of a combined Rankine-vapour-compression refrigeration cycle. *Energy Conversion and Management*, 51, 2557–2564. doi: 10.1016/j.enconman.2010.04.016
- [15] Cihan, E. (2014). Cooling performance investigation of a system with an organic Rankine cycle using waste heat sources. *Journal of Thermal Science and Technology*, 34(1), 101–109.
- [16] Bu, X., Wang, L., & Li, H. (2013). Performance analysis and working fluid selection for geothermal energy-powered organic Rankine-vapor compression air conditioning. *Geothermal Energy*, 1, 1–14. doi: 10.1186/2195-9706-1-2
- [17] Li, H., Bu, X., Wang, L., Long, Z., & Lian, Y. (2013). Hydrocarbon working fluids for a Rankine cycle powered vapor compression refrigeration system using low-grade thermal energy. *Energy and Buildings*, 65, 167–172. doi: 10.1016/j.enbuild.2013.06.012
- [18] Wang, H., Peterson, R., Harada, K., Miller, E., Ingram-Goble, R., Fisher, L., Yih, J., & Ward, C. (2011). Performance of a combined organic Rankine cycle and vapor compression cycle for heat activated cooling. *Energy*, 36, 447–458. doi: 10.1016/j.energy.2010.10.020
- [19] Yue, C., You, F., & Huang, Y. (2016). Thermal and economic analysis of an energy system of an ORC coupled with vehicle air conditioning. *International Journal of Refrigeration*, 64, 152–167. doi: 10.1016/j.ijrefrig.2016.01.005
- [20] Hu, B., Guo, J., Yang, Y., & Shao, Y. (2022). Performance analysis and working fluid selection of organic Rankine steam compression air conditioning driven by ship waste heat. *Energy Reports*, 8, 194–202. doi: 10.1016/j.egy.2022.01.094
- [21] Kim, K.H., & Perez-Blanco, H. (2015). Performance analysis of a combined organic Rankine cycle and vapor compression cycle for power and refrigeration cogeneration. *Applied Thermal Engineering*, 91, 964–974. doi: 10.1016/j.applthermaleng.2015.04.062
- [22] Khatoun, S., Almfrejji, N.M.A., & Kim, M.H. (2021). Thermodynamic study of a combined power and refrigeration system for low-grade heat energy source. *Energies*, 14(2), 410. doi: 10.3390/en14020410
- [23] Jeong, J., & Kang, Y.T. (2004). Cycle of a refrigeration cycle driven by refrigerant steam turbine. *International Journal of Refrigeration*, 27, 33–41. doi: 10.1016/S0140-7007(03)00101-4
- [24] Küçük, E., & Kılıç, M. (2023). Exergoeconomic and Exergetic Sustainability Analysis of a Combined Dual-Pressure Organic Rankine Cycle and Vapor Compression Refrigeration Cycle. *Sustainability*, 15(8), 6987. doi: 10.3390/su15086987
- [25] Wang, Z., Zhao, Y., Xia, X., Zhang, S., Xiao, Y., Zhang, X., & Chen, W. (2024). Experimental study of the thermodynamic performance of the ORC-VCC system with a zeotropic mixture. *Applied Thermal Engineering*, 250, 123534. doi: 10.1016/j.applthermaleng.2024.123534
- [26] Qureshi, F.M., Chandio, M.W., Memon, A.A., Kumar, L., & Awad, M.M. (2024). Thermal analysis of solar energy based organic Rankine cycle cascaded with vapor compression refrigeration cycle. *Energy Nexus*, 14, 100291. doi: 10.1016/j.nexus.2024.100291
- [27] Al-Sayyab, A.K.S., Mota-Babiloni, A., & Navarro-Esbrí, J. (2023). Performance Evaluation of Modified Compound Organic Rankine-Vapour Compression Cycle with Two Cooling Levels, Heating, and Power Generation. *Applied Energy*, 334, 120651. doi: 10.1016/j.apenergy.2023.120651
- [28] Mota-Babiloni, A., Navarro-Esbrí, J., Barragán, A., Molés, F., & Peris, B. (2014). Drop-in energy performance evaluation of R1234yf and R1234ze (E) in a vapor compression system as R134a replacements. *Applied Thermal Engineering*, 71, 259–265. doi: 10.1016/j.applthermaleng.2014.06.056
- [29] Calm, J.M., & Hourahan, G.C. (2011). Physical, safety, and environmental data summary for current and alternative refrigerants. *Proceedings of the 23rd International Congress of Refrigeration*, Prague, Czech Republic, 21–26 August 2011, ID 915.
- [30] Sokhansafat, T., Kasaeian, A., Rahmani, K., Heidari, A.H., Aghakhani, F., & Mahian, O. (2018). Thermo-economic and environmental analysis of solar flat plate and evacuated tube collectors in cold climatic conditions. *Renewable Energy*, 115, 501–508. doi: 10.1016/j.renene.2017.08.057
- [31] Li, P., Li, J., Pei, G., Munir, A., & Ji, J. (2016). A cascade organic Rankine cycle power generation system using hybrid solar energy and liquefied natural gas. *Solar Energy*, 127, 136–146. doi: 10.1016/j.solener.2016.01.029
- [32] Yaiche, M.R., Bouhanik, A., Bekkouche, S.M.A., Malek, A., & Benouaz, T. (2014). Revised solar maps of Algeria based on sunshine duration. *Energy Conversion and Management*, 82, 114–123. doi: 10.1016/j.enconman.2014.02.063
- [33] Macchi, E., & Perdichizzi, A. (1981). Efficiency Prediction for Axial-Flow Turbines Operating with Nonconventional Fluids. *Journal of Engineering for Power*, 103, 718–724. doi: 10.1115/1.3230794
- [34] Invernizzi, C., Iora, P., & Silva, P. (2007). Bottoming micro-Rankine cycles for micro-gas turbines. *Applied Thermal Engineering*, 27, 100–110. doi: 10.1016/j.applthermaleng.2006.05.003
- [35] Lakew, A.A., & Bolland, O. (2010). Working fluids for low-temperature heat source. *Applied Thermal Engineering*, 30, 1262–1268. doi: 10.1016/j.applthermaleng.2010.02.009
- [36] Stijepovic, M.Z., Linke, P., Papadopoulos, A.I., & Grujic, A.S. (2012). On the role of working fluid properties in Organic Rankine Cycle performance. *Applied Thermal Engineering*, 36, 406–413. doi: 10.1016/j.applthermaleng.2011.10.057